

# Hydrologic assessment of the TMPA 3B42-V7 product in a typical alpine and gorge region: the Lancang River basin, China

Zhaoli Wang, Jiachao Chen, Chengguang Lai, Ruida Zhong, Xiaohong Chen and Haijun Yu

## ABSTRACT

To evaluate the accuracy and applicability of the TMPA 3B42-V7 precipitation product for the Lancang River basin, we used different statistical indices to explore the performance of the product in comparison to gauge data. Then, we performed a hydrologic simulation using the Variable Infiltration Capacity (VIC) hydrological model with two scenarios (Scenario I: streamflow simulation using gauge-calibrated parameters; Scenario II: streamflow simulation using 3B42-V7-recalibrated parameters) to verify the applicability of the product. The results of the precipitation analysis show good accuracy of the V7 precipitation data. The accuracy increases with the increase of both space and time scales, while time scale increases cause a stronger effect. The satellite can accurately measure most of the precipitation but tends to misidentify non-precipitation events as light precipitation events (<1 mm/day). The results of the hydrologic simulation show that the VIC hydrological model has good applicability for the Lancang River basin. However, 3B42-V7 data did not perform as well under Scenario I with the lowest Nash–Sutcliffe coefficient of efficiency (NSCE) of 0.42; Scenario II suggests that the error drops significantly and the NSCE increases to 0.70 or beyond. In addition, the simulation accuracy increases with increased temporal scale.

**Key words** | hydrologic simulation, Lancang River, TMPA 3B42-V7 product, VIC model

**Zhaoli Wang**

**Jiachao Chen**

**Chengguang Lai** (corresponding author)  
School of Civil Engineering and Transportation,  
South China University of Technology,  
Guangzhou 510641, China;  
State Key Laboratory of Subtropical Building  
Science,  
South China University of Technology,  
Guangzhou 510641, China;  
and  
Guangdong Engineering Technology Research  
Center of Safety and Greenization for Water  
Conservancy Project,  
Guangzhou 510641, China  
E-mail: laichg@scut.edu.cn

**Ruida Zhong**

**Xiaohong Chen**

Center for Water Resources and Environment  
Research,  
Sun Yat-sen University,  
Guangzhou 510275, China

**Haijun Yu**

State Key Laboratory of Simulation and Regulation  
of Water Cycle in River Basin, Research Center  
on Flood and Drought Disaster Reduction of the  
Ministry of Water Resources,  
China Institute of Water Resources and  
Hydropower Research,  
Beijing 100038, China

## INTRODUCTION

Accurate precipitation data, especially featuring high accuracy and spatial-temporal resolution, are vital for hydrologic simulations, water resource management, flood and drought disaster forecasts, and other relevant studies (Collischonn *et al.* 2008; Hou *et al.* 2014). Currently, the traditional precipitation data are mainly obtained from gauge observations and ground-based radar measurements. However, the gauge measurement is typically affected by its spatial distribution as well as by the density of station networks (Li 2008; Li *et al.* 2013), whereas the data from ground-based radars are frequently impacted by the terrain and electronic signals. In such a case, it is still difficult to obtain completely reliable and

accurate precipitation data, even when spatial interpolation methods are used (Li 2008; Teegavarapu *et al.* 2012; Plouffe *et al.* 2015; Tesemma *et al.* 2015), especially for alpine and gorge regions (Yang *et al.* 2013).

Benefitting from technological progress, a series of high-resolution satellite-based precipitation products have been developed during recent decades, such as the Precipitation Estimation from Remotely Sensed Information using Artificial Neural Networks (PERSIANN) (Hsu *et al.* 1997), Tropical Rainfall Measuring Mission (TRMM) Multi-satellite Precipitation Analysis (TMPA) products (Huffman *et al.* 2007), Integrated Multi-satellite Retrievals for Global

Precipitation Measuring (IMERG) products (Hou *et al.* 2014), and the Climate Prediction Center Morphing (CMORPH) method (Joyce *et al.* 2004), which provide new data sources for hydrological and meteorological research. The TRMM, including TRMM Microwave Imager, Precipitation Radar, Visible and Infrared Radiometer, Clouds and Earth's Radiant Energy System, and Lighting Imaging System, was cooperatively designed and developed by the US National Aeronautics and Space Administration (NASA) and the Japan Aerospace Exploration Agency. Enormous amounts of data have been accumulated since the satellite was launched on November 28th, 1997 (Simpson *et al.* 1996; Huffman *et al.* 2007; Rui 2010). As the representative product of the TRMM, the TMPA 3B42 provides two products: the post-process TMPA 3B42 product and the near-real-time TMPA 3B42RT product. The post-process product and the near-real-time product enable a high spatial resolution of 0.25° and a coverage from 50°S-50°N to 60°S-60°N, respectively. The data of the near-real-time product are directly derived from satellites with slight calibration, using non-TRMM data obtained from multiple sensors, and thus they can be available in near-real time (about 9 h after the observation); the post-process product is re-calibrated from pure satellite estimates based on monthly surface rain gauge data, and hence it would be made public much later than 3B42RT (10–15 days after the end of each month) (Huffman *et al.* 2010). Under this circumstance, the 3B42 product can provide more accurate and reliable precipitation data.

The latest version of the 3B42 product, TMPA 3B42-V7 (hereafter simply referred to as V7), uses the latest version of the re-calibrated algorithm and was released in June 2012. The accuracy of the V7 product was generally improved and the bias for low latitude humid areas was reduced compared to the previous V6 version (Huffman *et al.* 2007, 2010; Li *et al.* 2013; Yong *et al.* 2014; Liu 2015; Prakash *et al.* 2015). The effects on hydrologic simulations of the V7 version are also considered to exceed those of the V6 version (Liu *et al.* 2012; Xue *et al.* 2013). Additionally, the V7 product has better performance in various measuring indices compared to CMORPH, PERSIANN, and Global Satellite Mapping of Precipitation (Guo *et al.* 2015; Salio *et al.* 2015; Duan *et al.* 2016). Still, the accuracy of the product needs to be improved because the satellite uses electromagnetic waves, which may be severely altered by precipitous terrain (Curtis *et al.* 2007; Aghakouchak

*et al.* 2009). Overall, the 3B42 products, especially the V7 version, have high application value and considerable development prospects. However, the data collection and precipitation inversion process are strongly influenced by many factors (e.g. topography and weather conditions); under this circumstance, the accuracy and applicability in certain specific regions need to be further investigated, especially for alpine and gorge regions (Liu *et al.* 2015).

For the hydrological utility, the 3B42 products have superior performance in basins with relatively plain terrain, including the Ganges-Brahmaputra River basin (Siddique-E-Akbor *et al.* 2014), the Amazon River basin (Collischonn *et al.* 2008), and the Gilgel Abay River basin (Bitew & Gebremichael 2011). Additionally, in a typical rainstorm area (Hu *et al.* 2013) and plateau and mountainous areas (Meng *et al.* 2014), TMPA 3B42 products also showed good performance. Current studies suggest that the TMPA 3B42 products feature wide-coverage applicability and have a good hydrologic model adaptation in most basins across the world. However, the hydrological utility of 3B42 products in a basin featuring typical alpine and gorge regions remains to be determined and tested. If the product still presents good hydrologic model adaptation in such a basin, it would have profound significance for the wide use of the V7 product.

As the seventh longest river in the world, the Lancang River (upstream of the Mekong River) originates from the Qinghai Province of China, successively flowing through the countries of Myanmar, Laos, Thailand, Cambodia, and Vietnam. The water resources of this river greatly affect the economic development and social stability of Southwest China and the Southeast Asian countries. Accordingly, it is necessary to master the changing hydrologic situation to legitimately develop the water resources. The Lancang River basin features extremely complex underlying surfaces, including plateaus, snowfields, steep mountains, and arduous canyons. The arduous canyons of the upper and middle reach constitute the renowned and typical 'V' type canyon. Limited by the adverse topography and climate, only a few national meteorological stations have been established in the basin until now; most of the national stations are located at low altitude and at easily accessible places, while the upper and middle reaches of the basin distribute bare sites, resulting in poor representation of the precipitation data (Zeng & Li 2011). Under this circumstance, searching spatially-continuous high-resolution

data and a reliable precipitation data source is of great importance for this basin. Considering the significant advantages and wide applications, the V7 data may be a good choice for this basin and could provide a potential tool for obtaining more accurate precipitation data. However, as mentioned before, most of the studies on TRMM were conducted in relatively flat and open terrain (Hu *et al.* 2013; Wang *et al.* 2017a) and studies that focused on areas with complex topography (especially in alpine and gorge regions) are comparatively rare. Under this circumstance, it remains a challenging topic whether the V7 data still fit well in the Lancang River basin with its formidable and complex natural conditions, and whether the hydrological utility driven by V7 data performs as well as that driven by traditional observed data.

Therefore, the objectives of this study are (1) to evaluate the accuracy and performance of the post-processed V7 product in the Lancang River basin and (2) to validate the applicability of the product via hydrologic simulation with the Variable Infiltration Capacity (VIC) model. This study offers effective tools for solving the problem of precipitation data deficiencies in the Lancang River basin, and provides a reference for the applications of the V7 product, especially for the applications in alpine and gorge regions.

## STUDY AREA AND DATA

### Study area

As a typical river that runs from north to south, the Lancang River originates in the Tanggula mountains north of China and flows across the Hengduan Mountains. The Lancang River basin covers 88,051 km<sup>2</sup> with an average annual runoff of  $30.6 \times 10^9$  m<sup>3</sup>. In contrast to its abundant hydrological and biological resources, the observational data of this basin are insufficient. The Lancang River (93°50' ~ 99°40'E, 25°30' ~ 33°50'N) flows across eight latitudes and can be characterized as a typical long-narrow basin shape. The river flows through many landform types, including plateaus and mountains that feature perennial snow cover, and gorge regions characterized by an average slope gradient of 4.2‰. The overall difference in elevation is more than 5,000 m from north to south, creating rich hydropower resources. Other features, such as the snow-melt water supply, three parallel rivers, and great change of

snowline, further add to the uniqueness of this basin in the world. Accordingly, the Lancang River basin can be a challenging study area for the V7 product.

As shown in Figure 1, this study divided the Lancang River basin into 188 grids with a resolution of 0.25°. A total of 19 meteorological stations were selected in and around the basin to provide observed meteorological data (gauge data). The JiuZhou hydrological station is located at the basin export (99°13'E, 25°47'N) and provides daily discharge data that can be used to verify hydrological simulations.

### Data

The V7 precipitation data can be downloaded from the official NASA website (<https://pmm.nasa.gov/data-access/downloads/trmm>). The observed daily data can be downloaded from the China Meteorological Data Service Center (<http://data.cma.cn/>), including data for 20–20-hour (i.e. from 20:00 to 20:00 of the next day) precipitation, air temperature, wind speed, sunshine hours, vapor pressure, and air pressure. We interpolated these gauge-based data to grid cells featuring a spatial resolution of 0.25° × 0.25° via the inverse distance weighting method for hydrological simulation.

The VIC model requires several model parameters, including land cover, topography, soil texture, and hydraulic parameters. The land cover data, which classify the land surface into 14 species, were derived from the global land cover file of the University of Maryland with 1 km resolution (Hansen *et al.* 1998). The topography parameters were derived from a high spatial resolution (90 m × 90 m) digital elevation model dataset measured by the Shuttle Radar Topography Mission (Jarvis *et al.* 2008). The soil texture parameters were provided by the Harmonized World Soil Database (Food and Agriculture Organization (FAO) 2009), and the soil hydraulic parameters were converted from the soil texture data by using Saxton's transformation formulas (Saxton & Rawls 2006).

## METHODOLOGY

### Precipitation comparison

In this study, the precipitation series of the Lancang River basin from 1998 to 2015 were selected, and the gauge data

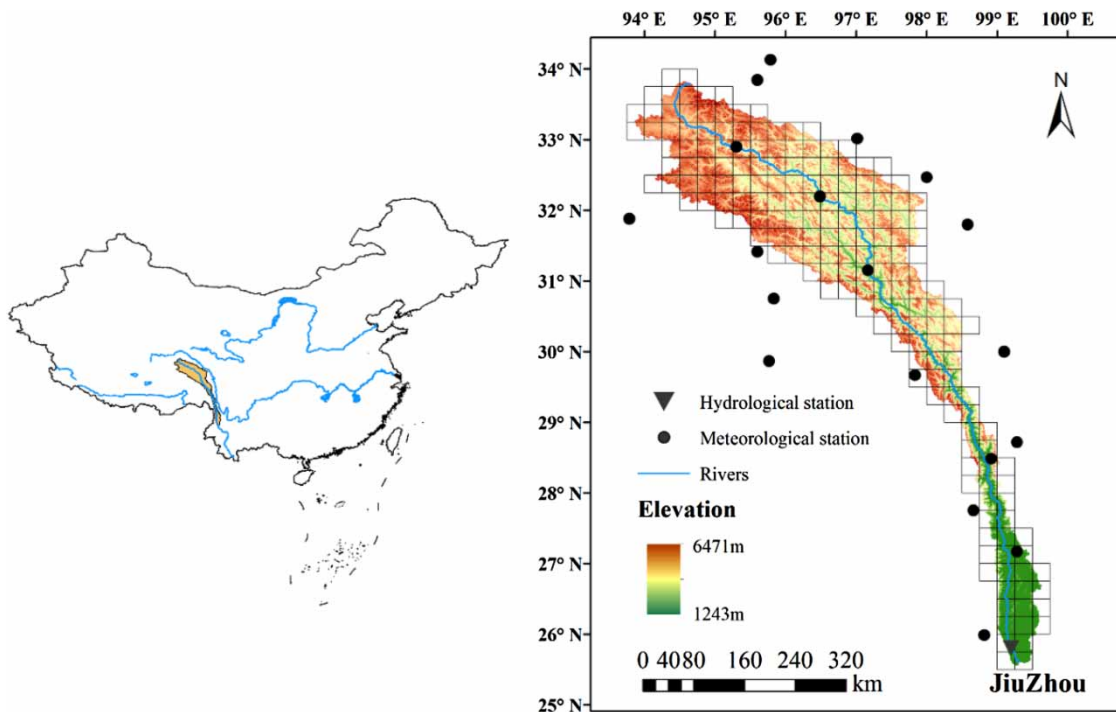


**Figure 1** | Geographic position and station distribution of the Lancang River basin.

were used as the actual value for a comparative analysis. Since satellite precipitation data errors are related to spatio-temporal scales, experiments will be conducted on daily scale, monthly scale, grid scale, and basin scale, respectively. The data recorded by the national meteorological stations can represent the precipitation of a certain region. For grid scale, the gauge data were compared with the nearest V7 grid data. The basin scale compares the precipitation data of all stations and grids in the basin after averaging them. Then, the occurrence frequency of daily precipitation in different rain intensity classes and its proportion of total precipitation are calculated to explore the characteristics of the V7 data.

### VIC hydrological model

This study used the VIC hydrological model (<http://vic.readthedocs.io/en/master/>) developed by Liang *et al.* (Liang *et al.* 1994; Liang & Xie 2001) to evaluate the hydrological utility of the V7 product. As a widely used hydrological model (Yong *et al.* 2010; Park & Markus 2014; Tesemma *et al.* 2015; Hengade & Eldho 2016; Mao *et al.* 2017; Wang *et al.* 2018), the VIC model is a grid-based macroscale distributed hydrological model that can simulate the land surface process based on

the water and energy balance and can consider several factors such as the heterogeneity of land cover and frozen soil. The VIC model typically divides soil into three layers in the vertical direction and is thus known as a VIC-3 L model, in which both the top and middle soil layers are used to represent the response of the soil moisture to rainfall events, while the bottom layer is used to represent the seasonal soil moisture characteristics. In the VIC model, the soil evapotranspiration and generation of surface runoff from upper soil layers are calculated based on the VIC curve, while the generation of the underground baseflow from the bottom soil layer is calculated based on the baseflow curve. Some soil parameters in the model, including the parameters  $b$ ,  $D_s$ ,  $D_{smax}$ ,  $W_s$ , and  $d_1 \sim d_3$ , are difficult to determine directly and thus, should be calibrated to obtain optimized values. An introduction to these parameters is listed in Table 1.

The latest version of the VIC model (VIC5.0) was chosen and requires several meteorological forcing data, including precipitation, air temperature, air pressure, wind speed, vapor pressure, longwave radiation, and shortwave radiation. Shortwave radiation can be converted from sunshine hours, and longwave radiation was calculated via

**Table 1** | List of the introduction to soil parameters that need to be calibrated

Variable name	Units	Description	Influence
$b$	–	Variable infiltration curve parameter (binfilt)	The generation of the surface runoff
$D_s$	–	Fraction of $D_{smax}$ where non-linear baseflow begins	The generation of the surface runoff
$D_{smax}$	mm/day	Maximum velocity of baseflow	The generation of the baseflow
$W_s$	–	Fraction of maximum soil moisture where non-linear baseflow occurs	The generation of the baseflow
$d_1$	m	Thickness of the first soil moisture layer	The evapotranspiration and the generation of the surface runoff and baseflow
$d_2$	m	Thickness of the second soil moisture layer	The evapotranspiration and the generation of the surface runoff and baseflow
$d_3$	m	Thickness of the third soil moisture layer	The evapotranspiration and the generation of the surface runoff and baseflow

conversion formula (Konzelmann *et al.* 1994) using temperature and vapor pressure.

Since the VIC model only calculates the runoff yield individually in a single grid cell, it is necessary to use the confluence model developed by Lohmann *et al.* (Lohmann *et al.* 1996). This model is based on the unit hydrograph method and the linearized Saint-Venant equation and can simulate the streamflow process to the basin outlet.

### Hydrological simulation scenarios

To evaluate the hydrological utility of the V7 product, it is necessary to perform a hydrological validation. The following two scenarios were performed to simulate the hydrological utility of the V7 precipitation product based on the parameters obtained from different precipitation products.

Scenario I (static parameter method): Input the rain gauge precipitation data into the VIC model and obtain a set of optimal parameters after calibration; then, apply the parameters to the V7-driven hydrological model. Under this scenario, the hydrological model is calibrated based on the gauge data and suits when the basins have sufficient measured hydrological data.

Scenario II (dynamic parameter method): Perform the calibration and validation based only on the V7 precipitation data. This scenario suits when the gauge data are insufficient and thus only uses satellite precipitation data to drive the hydrological model.

In this study, the period of 1998–1999 was set as the start-up period and it was thus not included for calculating

the statistical indices. The period of 2000–2002 was set as the calibration period and the period of 2003–2006 was set as the validation period.

### Statistical indices

The V7 product was evaluated using several statistical indices including the Pearson correlation coefficient (CC), the relative bias (BIAS), the root mean square error (RMSE), the probability of detection ( $R_D$ ), the false alarm ratio ( $R_{FA}$ ), and the normalized mean square error (NMSE) (Torgo 2017). The CC is used to evaluate the consistency between the V7 data and the gauge data; the BIAS describes the systematic deviation of the V7 data; the RMSE is used to measure the degree of the deviation between V7 data and gauge data; in other words, the RMSE can evaluate the accuracy of the satellite measurements.  $R_D$  is used to describe the probability that V7 detects a precipitation event correctly.  $R_{FA}$  is a ratio measuring whether V7 did not detect a precipitation event. The NMSE reflects the accuracy of the V7 data after considering the inherent deviation of the gauge data. In general, the estimations would be regarded as unavailable for a NMSE above 1.0 (Yao & Tan 2000).

The results of the hydrologic simulation were evaluated using CC, BIAS, and Nash–Sutcliffe coefficient of efficiency (NSCE) (Nash & Sutcliffe 1970). The NSCE is used to assess the degree of deviation between the simulated and the observed streamflow. The formulas of the statistical accuracy indices are listed in Table 2.

**Table 2** | List of the formulas of the statistical indices to quantify the performance of 3B42-V7 data

Statistical accuracy indices	Abbreviation	Units	Formula	Perfect value
Pearson correlation coefficient	CC	—	$CC = \frac{cov(P, S)}{\sqrt{var(P) \cdot var(S)}}$	1
Relative bias	BIAS	%	$BIAS = \frac{\sum_{i=1}^n S_i - \sum_{i=1}^n P_i}{\sum_{i=1}^n P_i} \times 100\%$	0
Root mean square error	RMSE	mm	$RMSE = \sqrt{\frac{1}{n} \sum_{i=1}^n (S_i - P_i)^2}$	0
Probability of detection	$R_D$	—	$R_D = \frac{n_{11}}{n_{11} + n_{10}}$	1
False alarm ratio	$R_{FA}$	—	$R_{FA} = \frac{n_{01}}{n_{11} + n_{01}}$	0
Normalized mean square error	NMSE	—	$NMSE = \frac{\frac{1}{n} \sum_{i=1}^n (S_i - P_i)^2}{var(P)}$	0
Nash–Sutcliffe coefficient of efficiency	NSCE	—	$NSCE = 1 - \frac{\frac{1}{n} \sum_{i=1}^n (S_i - P_i)^2}{var(P)}$	1

Note:  $P$ , gauge data series;  $S$ , 3B42-V7 data series;  $cov(P, S)$ , the covariance between  $P$  and  $S$ ;  $var(P, S)$ , the variance of  $P$  or  $S$ ;  $n$ , the length of  $P$  and  $S$  series;  $n_{11}$ , number of rainfall events that gauge recorded and 3B42-V7 detected;  $n_{10}$ , number of rainfall events that gauge recorded but 3B42-V7 did not detect;  $n_{01}$ , number of rainfall events that 3B42-V7 detected but gauge did not record.

## RESULTS AND ANALYSIS

### Evaluation of the 3B42-V7 data compared to the gauge data

A regression analysis and a detection performance analysis were conducted on different temporal scales (daily and monthly) and spatial scales (grid and basin). A regression analysis was performed (Figure 2) and the results of statistical indices are presented in Table 3.

As the results show, on a daily scale, the satellite data overestimate the overall amount of rainfall, and the poor linear relationships between gauge data and the nearest 3B42 grid data resulted in the CC from 0.37 to 0.55. For the precipitation detection capability, the TRMM satellites generally achieve good performance in the study area ( $R_D = 0.79$ ). However, the high  $R_{FA}$  ( $R_{FA} = 0.30$ ) indicates that the satellites may be overly sensitive to precipitation and can easily misidentify non-precipitation events as precipitation events. The low RMSEs indicate that the V7 data and the gauge measurement have small cumulative errors in the long-term series. The BIAS dropped significantly on the basin scale, indicating that the total

precipitation from both sources are fairly close. Compared to the grid scale, the V7 data show a better linear relationship and the NMSE reached 0.82 on the basin scale, indicating that the V7 data are more applicable on the basin scale. On a monthly scale, the satellite data overestimate the rainfall amount in general. With the enlargement of the time scale, the CC is greatly improved because the increased time scale covers the individual errors and the NMSEs also decrease sharply. Thus, the accuracy and consistency between the V7 data and the gauge data are further improved as the time scale expands (from daily to monthly), which may be due to the calibration of V7 data using monthly gauge data.

The occurrence frequency and the contributions to the total rainfall amount distribution of the daily precipitation in different rain intensity classes were calculated and compared between the gauge data and the V7 data both on grid and basin scale (Figure 3), respectively. Apparently, the satellite can precisely measure most of the occurred rainfall (>1 mm/day), which contributes more than 90% of the precipitation for the total rainfall. Associated with the  $R_{FA}$ , the V7 data mainly treat non-precipitation events as light precipitation events (0–1 mm/day).

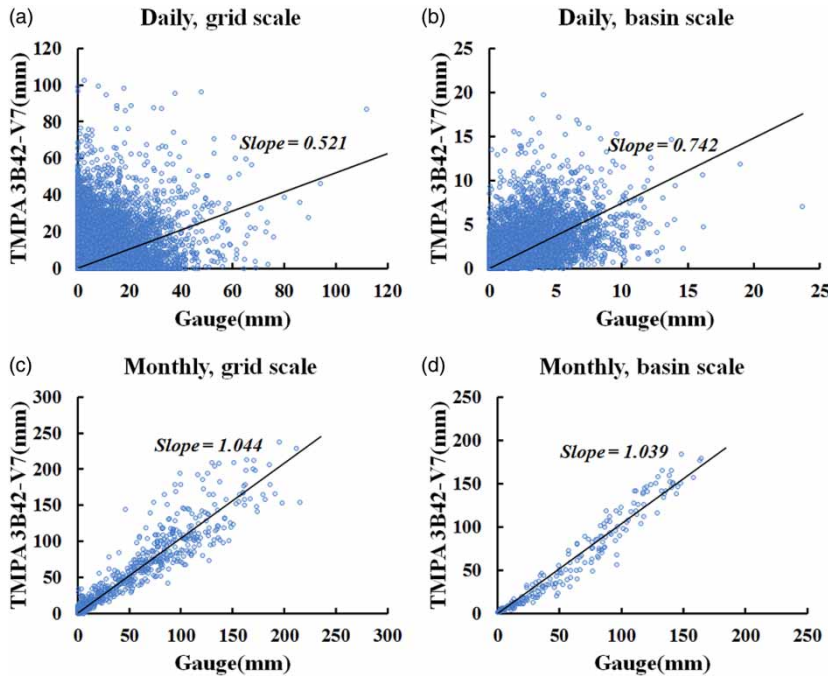


Figure 2 | Scatterplots of the precipitation comparison at two different spatial and temporal scales.

Table 3 | Statistical accuracy indices between 3B42-V7 and gauge data

Statistics	Grid scale						Basin scale					
	CC	BIAS	RMSE	NMSE	R <sub>D</sub>	R <sub>FA</sub>	CC	BIAS	RMSE	NMSE	R <sub>D</sub>	R <sub>FA</sub>
Daily	0.37	36.16	5.72	1.48	0.79	0.30	0.55	0.16	2.40	0.82	1	0.19
Monthly	0.88	36.16	32.56	0.29	1	0.03	0.98	0.16	12.00	0.07	1	0

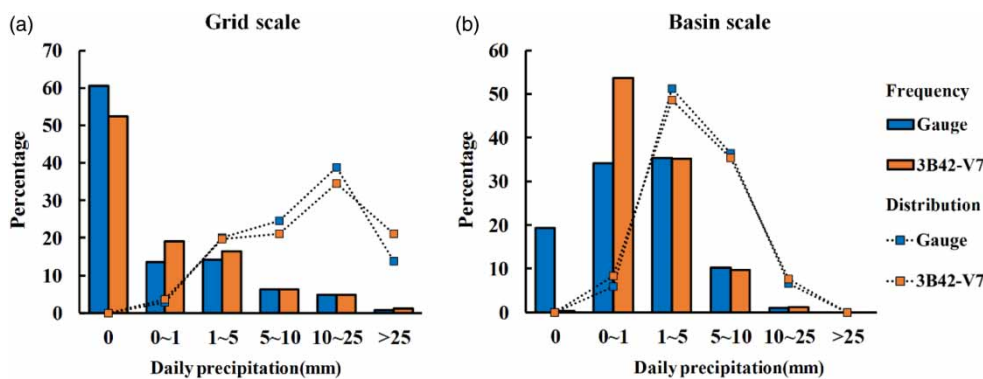


Figure 3 | Distribution of daily precipitation in different rain intensity classes and their relative contributions to the total rainfall amount on (a) grid and (b) basin scale.

Fortunately, the consequences of such errors are not severe since light precipitation only accounts for a small part (<10%) of the total precipitation in this region. In

terms of the distribution of precipitation contribution, the precipitation from both gauge data and V7 data are fairly consistent.

In summary, in comparison to other basins (Hu *et al.* 2013; Meng *et al.* 2014), the comprehensive complex terrains located in the Lancang River affect the measurement accuracy of the satellite product to some extent, and the consistency of the daily result on the grid scale is quite poor. Nevertheless, the overall quality of the product can still meet the accuracy required for engineering applications, especially for the application of the basin scale, which may benefit from the strong calibration capabilities of the satellite inversion algorithm. Additionally, the data accuracy can be greatly improved by enlarging the spatial or temporal scales.

### Hydrologic validation with the VIC model

#### Scenario I: static parameter method

The recorded results of the daily streamflow simulation during calibration and validation periods of the two scenarios are presented in Table 4, while the monthly streamflow simulation results are shown in Table 5.

As shown in Figure 4(a) and 4(b), on a daily scale, after calibrating with the gauge data (Scenario I), the VIC model performs well with the CC maintaining 0.86 and the NSCE exceeding 0.70 during the calibration and validation periods, respectively. This indicates that the simulation

results are sufficiently consistent with the observational data. Additionally, the BIAS values remain within an acceptable level of 8.56% and 2.03% for the calibration and validation periods, respectively, which indicates low deviation. Even so, there is still a gap between the simulation results and the observations due to various factors, including the wide span of latitude and altitude, the complexity of the terrain (e.g. plateau, alpine, and gorge), and the sparse gauge network with poor data representation. As shown in Table 4, the NSCE value is 0.73 at the calibration period and 0.74 at the validation period, which still reaches satisfactory performance. Therefore, the VIC hydrological model can still play an effective role in the Lancang River basin, even though the V7 data performance is significantly affected by snowmelt and its narrow shape.

After replacing the precipitation input data with the V7 data, the CCs slightly increase, while the BIAS values increase to 37.39% and 25.98% for the calibration and validation period, respectively. This indicates that the simulation results based on the parameters calibrated by gauge data significantly overestimate the runoff volume. The NSCEs are only 0.42 and 0.64 for the calibration and validation periods, respectively, which also confirms the poor performance of the V7 data under Scenario I. Under this circumstance, a high deviation may occur if the streamflow is still directly simulated using

**Table 4** | Accuracy indices of daily observed and simulated streamflow under two calibration scenarios

Periods	Precipitation products	Scenario I			Scenario II		
		CC	BIAS(%)	NSCE	CC	BIAS(%)	NSCE
Calibration	Gauge	0.86	8.56	0.73	—	—	—
	3B42-V7	0.88	37.39	0.42	0.86	11.58	0.70
Validation	Gauge	0.86	2.03	0.74	—	—	—
	3B42-V7	0.89	25.98	0.64	0.86	-4.58	0.72

**Table 5** | Accuracy indices of monthly observed and simulated streamflow under two calibration scenarios

Periods	Precipitation products	Scenario I			Scenario II		
		CC	BIAS (%)	NSCE	CC	BIAS (%)	NSCE
Calibration	Gauge	0.95	8.47	0.90	—	—	—
	3B42-V7	0.96	37.24	0.56	0.95	11.57	0.88
Validation	Gauge	0.93	2.06	0.85	—	—	—
	3B42-V7	0.94	25.86	0.75	0.94	-4.55	0.84



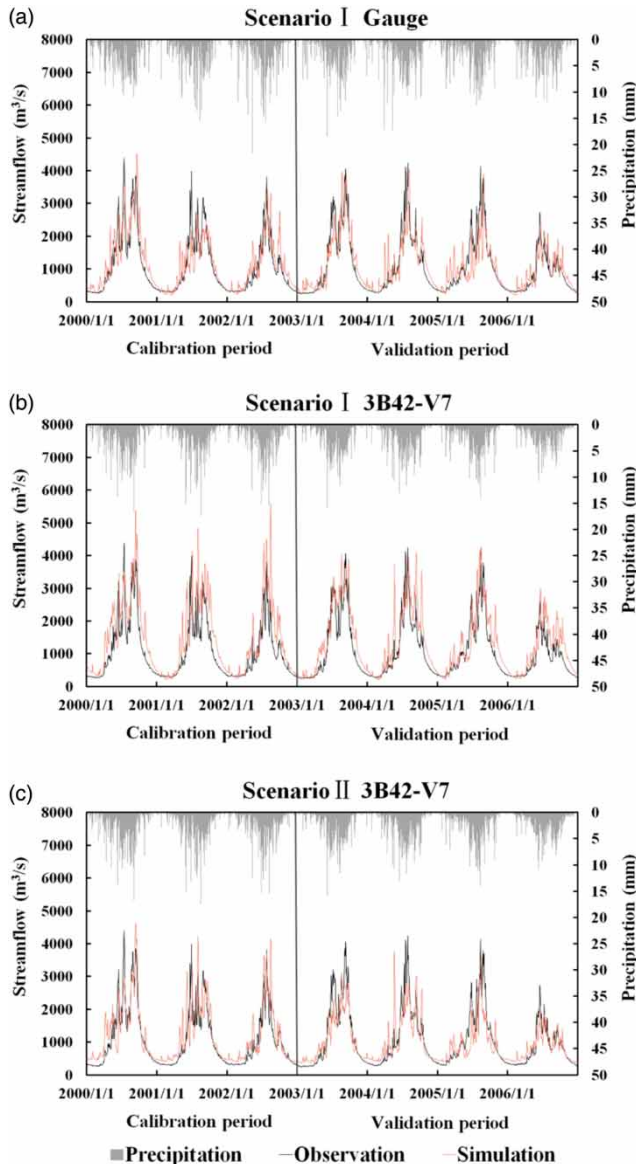


**Figure 4** | Daily simulated and observed hydrographs at JiuZhou station.

this set of parameters calibrated with the daily gauge precipitation data. Therefore, the parameters obtained in Scenario I are not suitable for the V7 precipitation data.

On a monthly scale, the accuracy of the streamflow simulation results based on the gauge is further improved. The CCs are above 0.90, and the NSCEs in the calibration and validation period are 0.90 and 0.85, respectively. Generally, the accuracy of the NSCEs is higher than that suggested by Moriasi *et al.* (2007). This further supports the applicability of the VIC model to the Lancang River basin.

However, although the accuracy of the streamflow simulation results increases with extended temporal scale, the results shown in Table 5 indicate that simply replacing the precipitation input file with the V7 data and simulating without changing the parameters will result in a large deviation. As shown in Figure 5(b), the streamflow simulation value is higher than the measured value.

### Scenario II: dynamic parameter method

To fully use the V7 data, we recalibrated the VIC hydrologic model with the V7 daily data. As shown in Figure 4(c),

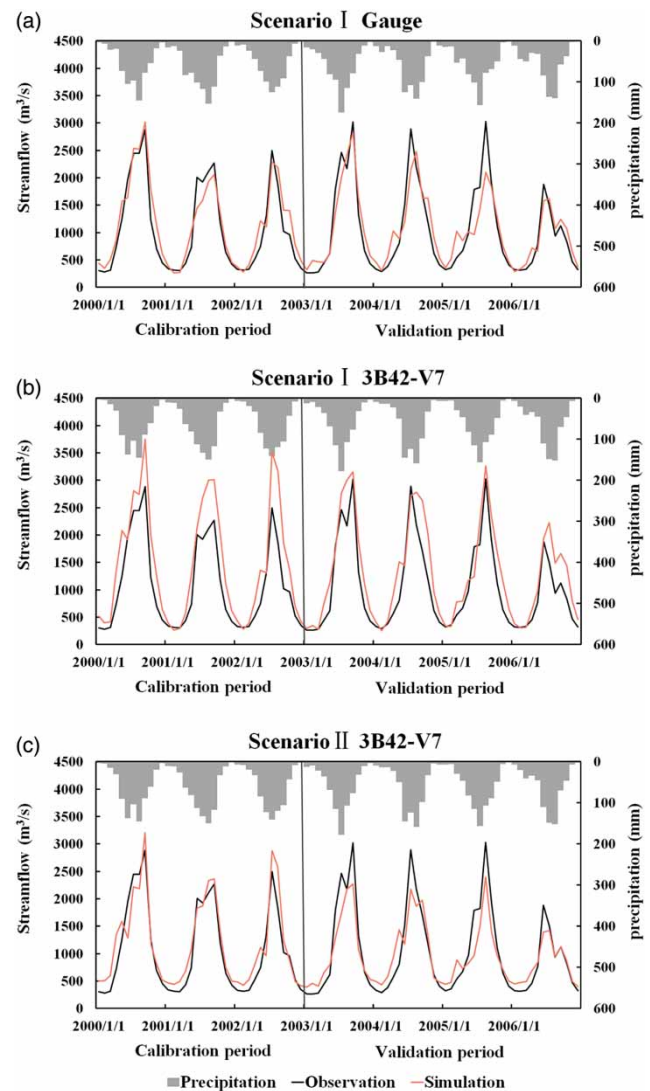


**Figure 5** | Monthly simulated and observed hydrographs at JiuZhou station.

under Scenario II, the V7 product can properly simulate the moderate level streamflow ( $1,000\text{--}2,000\text{ m}^3/\text{s}$ ), can indicate the periods of flood peaks, and can precisely capture several peak values. However, simulated values below  $1,000\text{ m}^3/\text{s}$  are generally higher than the observed values, and some peak flows are usually underestimated. The data in Table 4 indicate that the systematic bias significantly decreases after recalibration, with BIAS values decreasing to 11.58% and  $-4.58\%$  for the calibration and validation periods, respectively, while the CC values return to 0.86 (the same as the gauge-based simulation result) and the NSCEs return to a level above 0.70. All the changes of these indices lead to the conclusion that the accuracy of the daily simulation based on the V7 precipitation product is comparable to that obtained in other basins (Khan *et al.* 2011; Xue *et al.* 2013; Hao *et al.* 2014). Therefore, in light of the good simulation results based on the V7 data (the accuracy is close to the simulation result based on the gauge data), the V7 product has the ability to replace the gauge observation and can be used to perform a successful hydrological simulation in the Lancang River basin.

On a monthly scale, due to the enlargement of the temporal scale (from daily to monthly), the individual deviation of the V7 precipitation data is compensated and the simulation accuracy is further improved. Although some problems still remain, such as the underestimation of peak flow, or the slightly overestimated dry season, the data in Table 5 show that the CCs still exceed 0.94, and the NSCEs in the calibration and validation period are 0.88 and 0.83, respectively. Therefore, the V7 precipitation data achieved good hydrological utility on both daily scale and monthly scale.

## DISCUSSION

High-mountain gorge areas are always challenging for data acquisition via TRMM and other meteorological satellites, and the application of uncertainty analysis has always attracted the interest of scholars (Zeng & Li 2011; Zeng *et al.* 2012; Meng *et al.* 2014; Tong *et al.* 2014). The study area, the Lancang River basin, features high mountains, gorges, permafrost, and snow-covered areas; moreover, the meadow layer and the weathered layer at the source of the

river have strong permeability, thus creating great difficulties for the evaluation of the satellite precipitation product and hydrological simulation. For the product selection, only the latest post-process V7 product was chosen to conduct simulations, after considering that the accuracy of the real-time version product is generally lower than that of the post-process product. Furthermore, the products of 3B42 RTV5, RTV6, and RTV7 are not suitable for streamflow simulation in the upper Yangtze and Yellow River basins (Hao *et al.* 2014) that neighbor our study area. For hydrological model selection, Zulkafli *et al.* (2014) reported that the selection of hydrological models is important because it affects whether the variations of runoff peaks can be accurately simulated, especially in mountainous environments. We finally chose the VIC model to simulate the streamflow because it features strong functions; i.e. (1) it performs well in areas of complex topography; (2) it divides the soil into three layers and fully considers infiltration; and (3) the snow module in the model can fully consider the snowmelt situation. Therefore, the model offers a certain advantage of theoretical mechanism to simulate the streamflow in the complex basin. The VIC model, beyond all doubt, provides exactly the required tools for the challenges located in the study area, and finally, a good simulation result was achieved with this model.

According to the accuracy analysis, the satellite tends to mistake non-precipitation events for light precipitation events, which results in a high  $R_{FA}$ . According to a relevant study in other alpine and gorge regions, the  $R_{FA}$  tends to increase with increasing elevation. In the study of Yang *et al.* (2013), the average  $R_{FA}$  of the 3B42-V6 product for the Jinsha River basin (elevation: 263–5,910 m) was above 0.6. However, the  $R_{FA}$  of the V7 product in the Lancang River basin (elevation: 1,243–6,471 m) was only 0.3, which indicates that the V7 data are more suitable for alpine and gorge regions than the V6 data. The quality of satellite precipitation data can be improved with the advancement of observation techniques and the improvement of the inversion algorithm. However, the problems of the representativeness of gauge observation data and the difficulty of the station maintenance are limited by natural conditions, and they cannot be solved in a short time. Under this circumstance, it is of great significance to evaluate the accuracy and hydrological utility of the V7 product in the Lancang

River basin featuring complex terrain and sparsely distributed meteorological stations.

For hydrological simulation, Jiang *et al.* (2014) found that the 3B42 product is able to simulate low and medium level streamflow well, while underestimating flow peaks; Sun *et al.* (2016) also formed a similar conclusion in their study. However, the performance of the model for the Lancang River basin is significantly different; specifically, the V7 precipitation data not only underestimate some extreme flow peaks, but also overestimate the dry season streamflow. The reason why the V7 product underestimates the flow peaks may be related to the high  $R_{FA}$ . The hydrologic simulation result of the neighboring regions may provide a reference for this study. The upper Yellow River and the upper Yangtze River, together with the Lancang River basin are located on the Tibetan Plateau with high elevation and sparse meteorological stations. The difference is that the topography of the Lancang River basin is more complicated. Hao *et al.* (2014) used the VIC model to assess the hydrological utility of the 3B42 precipitation products in the upper Yellow River and the upper Yangtze River. The streamflow simulation results based on the post-process version show that the NSCEs from both basins fluctuate around 0.6, and daily streamflow simulation can be performed based on the 3B42 post-process product. The streamflow simulation results of Scenario II in this study show that the NSCEs reach above 0.7 and have a good hydrological effect on daily scale, which exceeds those of the upper Yellow River and upper Jinsha River. The difference may be caused by the usage of different versions of the hydrological models; i.e., the newest version (i.e. VIC5.0) could obtain much better effects than older versions (VIC 4.0 or earlier). More comprehensive meteorological data (e.g. radiation and vapor pressure) added to the VIC5.0 achieved simulation results that were closer to the true value and thus greatly improved simulation accuracy. Additionally, Tong

*et al.* (2014) used gauge-calibrated model parameters to preliminarily evaluate the hydrological utility of different satellite precipitation products in the upper Yellow and upper Yangtze River basins neighboring our study area. In our study, we further evaluated the hydrological utility of the V7 with two scenarios and found that after the model was recalibrated by V7, the hydrological simulation results significantly improved. Hence, the V7 product can be regarded as an ideal supplement for the precipitation data in alpine and gorge regions although the aggregate performance is inferior to the plain area (Hu *et al.* 2013; Wang *et al.* 2017a).

Table 6 lists some VIC model parameters. We found that, to reduce the simulation bias, the  $d_2$  increased while  $b$  decreased after recalibration, which indicates that soil evaporation would increase while surface runoff would decrease, thus resulting in more baseflow. Therefore, the underestimation of the flow peaks by V7 may mainly result from the increased evaporation and the decreased surface runoff, while the overestimation of the baseflow may mainly result from the decreased  $b$  and an underestimation of the frequency of the non-precipitation in the upper reaches of the Lancang River. Based on the above analysis, it is not a wise choice to use the V7 data for drought warning in the upstream area of the Lancang River because the overestimated baseflow during the dry season might decrease the drought level and lead to an underestimation of the severity of the disaster.

In general, the quality of satellite precipitation products is mainly affected by both topography and precipitation magnitude (<1 mm/day or >25 mm/day). Given the good accuracy and hydrological utility of the V7 product in the typical rainstorm (Hu *et al.* 2013), alpine, and gorge areas, it can be speculated that the V7 precipitation product has been developed to a mature stage and can be applied to most areas with good results. The coverage observation

**Table 6** | The calibrated parameters of the VIC model under two scenarios

Scenarios	Variable name						
	$b$	$Ds$	$Ds_{max}$	$Ws$	$d_1$	$d_2$	$d_3$
I	0.5500	0.1250	29.2356	0.9309	0.1000	0.3382	0.4375
II	0.2986	0.0493	12.1488	0.6566	0.1000	0.5618	0.4750

will also become a trend to compensate the insufficiency of gauge observations and even become a main approach to monitor precipitation, especially in alpine and gorge regions. With the development of remote sensing technology, the technical problems of precipitation observations in complex terrain, such as in alpine and gorge areas, are expected to be overcome (Tang et al. 2016); the accuracy and application effects are also anticipated to be further improved. Since the GPM (Global Precipitation Measurement), i.e. the successor of the TRMM, has significant improvements in the ability to detect the light and solid precipitation (Huffman et al. 2012), the next generation IMERG product might provide an even better precipitation estimation and hydrological utility (Wang et al. 2017b).

## CONCLUSIONS

This study first evaluated the accuracy and performance of the post-processed V7 product for the Lancang River basin featuring formidable and complex natural conditions. Subsequently, the applicability of the product via hydrological simulation using the VIC model at the study area was validated. The accuracy of the V7 daily precipitation data on grid scale is quite poor. Nevertheless, the statistical indices are greatly improved and the data can be applied (with  $NMSE = 0.82 < 1.0$ ) in combination with the spatial enlargement from grid scale to basin scale. In addition, the data accuracy was further improved with the enlargement of the time scale (from daily to monthly). Some errors mainly occurred for light precipitation; specifically, the data mistake non-precipitation events as light precipitation events ( $< 1$  mm/day). Fortunately, the V7 data can accurately capture most rainfall events ( $> 1$  mm/day) which contribute to over 90% of the total precipitation. Moreover, the distributions of the V7 data in different rain intensities are close to the gauge data. The overall quality of the product still meets the accuracy required for engineering applications.

The VIC model has good applicability to the Lancang River basin, which is a typical narrow-shaped and complex basin where even snow is present. The direct application of the V7 data to the VIC model based on the calibration of gauge data clearly leads to a higher runoff level and

causes larger deviation. After recalibrating the hydrologic model with the V7 data, the medium level flow simulation then becomes more accurate and some of the flood peaks are also accurately captured. In general, the accuracy of the V7-based simulation is similar to that of the gauge-based results, and the enlargement of the temporal scale can further improve simulation accuracy. Therefore, the V7 product can become a new source of precipitation data for the Lancang River basin and thus has great potential for the hydrological simulation.

## ACKNOWLEDGEMENTS

The research is financially supported by the National Natural Science Foundation of China (Grant No. 51579105, 51709117, 91547202, 51479216); China Postdoctoral Science Foundation (2017M612662); the Science and Technology Program of Guangzhou City (201707010072); the Science and Technology Planning Project of Guangdong Province, China (2017A040405020); and the Special Fund of Water Resources Conservation and Protection of Guangdong Province (2017).

## REFERENCES

- Aghakouchak, A., Nasrollahi, N. & Habib, E. 2009 Accounting for uncertainties of the TRMM satellite estimates. *Remote Sensing* **1** (3), 606–619.
- Bitew, M. M. & Gebremichael, M. 2011 Evaluation of satellite rainfall products through hydrologic simulation in a fully distributed hydrologic model. *Water Resources Research* **47** (W06526).
- Collischonn, B., Collischonn, W. & Tucci, C. E. M. 2008 Daily hydrological modeling in the Amazon basin using TRMM rainfall estimates. *Journal of Hydrology* **360** (14), 207–216.
- Curtis, S., Crawford, T. W. & Lecce, S. A. 2007 A comparison of TRMM to other basin-scale estimates of rainfall during the 1999 Hurricane Floyd flood. *Natural Hazards* **43** (2), 187–198.
- Duan, Z., Liu, J., Tuo, Y., Chiogna, G. & Disse, M. 2016 Evaluation of eight high spatial resolution gridded precipitation products in Adige Basin (Italy) at multiple temporal and spatial scales. *Science of the Total Environment* **573**, 1536–1553.
- FAO 2009 *Harmonized World Soil Database*. FAO Land & Water Digital Media.
- Guo, H., Chen, S., Bao, A., Hu, J., Gebregiorgis, A., Xue, X. & Zhang, X. 2015 Inter-comparison of high-resolution satellite

- precipitation products over Central Asia. *Remote Sensing* **7** (6), 7181–7211.
- Hansen, M., DeFries, R., Townshend, J. R. G. & Sohlberg, R. 1998 *UMD Global Land Cover Classification, 1 Kilometer, 1.0*. Department of Geography, University of Maryland, College Park, Maryland, 1981–1994.
- Hao, Z. C., Tong, K., Liu, X. L. & Zhang, L. L. 2014 Capability of TMPA products to simulate streamflow in upper Yellow and Yangtze River basins on Tibetan Plateau. *Water Science and Engineering* **82** (3), 237–249.
- Hengade, N. & Eldho, T. I. 2016 Assessment of LULC and climate change on the hydrology of Ashti Catchment, India using VIC model. *Journal of Earth System Science* **125** (8), 1623–1634.
- Hou, A. Y., Kakar, R., Neeck, S., Azarbarzin, A. A., Kummerow, C. D., Kojima, M., Oki, R., Nakamura, K. & Iguchi, T. 2014 The Global Precipitation Measurement (GPM) mission. *Bulletin of the American Meteorological Society* **95** (5), 701–722.
- Hsu, K. L., Gao, X. G., Sorooshian, S. & Gupta, H. V. 1997 Precipitation estimation from remotely sensed information using artificial neural networks. *Journal of Applied Meteorology* **36** (9), 1176–1190.
- Hu, Q. F., Yang, D. W., Wang, Y. T. & Yang, H. B. 2013 Accuracy and spatio-temporal variation of high resolution satellite rainfall estimate over the Ganjiang River Basin. *Science China Technological Sciences* **56** (4), 853–865.
- Huffman, G. J., Adler, R. F., Bolvin, D. T., Gu, G., Nelkin, E. J., Bowman, K. P., Stocker, E. & Wolff, D. B. 2007 The TRMM Multi-satellite Precipitation Analysis (TMPA): quasi-global precipitation estimates at fine scales. *Journal of Hydrometeorology* **38** (8), 22–55.
- Huffman, G. J., Adler, R. F., Bolvin, D. T. & Nelkin, E. J. 2010 The TRMM Multi-Satellite Precipitation Analysis (TMPA). In: *Satellite Rainfall Applications for Surface Hydrology* (M. Gebremichael & F. Hossain, eds). Springer, Dordrecht, pp. 3–22.
- Huffman, G. J., Bolvin, D. T., Braithwaite, D., Hsu, K., Joyce, R., Kidd, C., Sorooshian, S., Xie, P. & Yoo, S.-H. 2012 Developing the integrated multi-satellite retrievals for GPM (IMERG). *Acta Paulista De Enfermagem* **25** (1), 146–150.
- Jarvis, A., Reuter, H. I., Nelson, A. & Guevara, E. 2008 Hole-filled seamless SRTM data V4, International Centre for Tropical Agriculture (CIAT).
- Jiang, S., Ren, L., Yong, B., Yuan, F., Gong, L. & Yang, X. 2014 Hydrological evaluation of the TRMM multi-satellite precipitation estimates over the Mishui basin. *Advances in Water Science* **25** (5), 641–649.
- Joyce, R. J., Janowiak, J. E., Arkin, P. A. & Xie, P. 2004 CMORPH: A method that produces global precipitation estimates from passive microwave and infrared data at high spatial and temporal resolution. *Journal of Hydrometeorology* **5** (3), 287–296.
- Khan, S. I., Adhikari, P., Hong, Y., Vergara, H., Adler, R. F., Policelli, F., Irwin, D., Korme, T. & Okello, L. 2011 Hydroclimatology of Lake Victoria region using hydrologic model and satellite remote sensing data. *Hydrology and Earth System Sciences* **15** (1), 107–117.
- Konzelmann, T., van de Wal, R. S. W., Greuell, W., Bintanja, R., Henneken, E. A. C. & Abe-Ouchi, A. 1994 Parameterization of global and longwave incoming radiation for the Greenland ice sheet. *Global & Planetary Change* **9** (1–2), 143–164.
- Li, J. 2008 A review of spatial interpolation methods for environmental scientists. *Record – Geoscience Australia* **137**, 1–137.
- Li, Z., Yang, D. & Hong, Y. 2013 Multi-scale evaluation of high-resolution multi-sensor blended global precipitation products over the Yangtze River. *Journal of Hydrology* **500**, 157–169.
- Liang, X. & Xie, Z. 2001 A new surface runoff parameterization with subgrid-scale soil heterogeneity for land surface models. *Advances in Water Resources* **24** (9), 1173–1193.
- Liang, X., Lettenmaier, D. P., Wood, E. F. & Burges, S. J. 1994 A simple hydrologically based model of land surface water and energy fluxes for general circulation models. *Journal of Geophysical Research Atmospheres* **99** (D7), 14415–14428.
- Liu, Z. 2015 Comparison of versions 6 and 7 3-hourly TRMM multi-satellite precipitation analysis (TMPA) research products. *Atmospheric Research* **163**, 91–101.
- Liu, J., Zhu, A. & Duan, Z. 2012 Evaluation of TRMM 3b42 precipitation product using rain gauge data in Meichuan Watershed, Poyang Lake Basin, China. *Journal of Resources and Ecology* **3** (4), 359–366.
- Liu, M., Xu, X., Sun, A. Y., Wang, K., Yue, Y., Tong, X. & Liu, W. 2015 Evaluation of high-resolution satellite rainfall products using rain gauge data over complex terrain in southwest China. *Theoretical and Applied Climatology* **119** (1), 203–219.
- Lohmann, D., Nolte Holube, R. & Raschke, E. 1996 A large-scale horizontal routing model to be coupled to land surface parametrization schemes. *Tellus Series A-Dynamic Meteorology & Oceanography* **48** (5), 708–721.
- Mao, Y., Wu, Z., He, H., Lu, G., Xu, H. & Lin, Q. 2017 Spatio-temporal analysis of drought in a typical plain region based on the soil moisture anomaly percentage index. *Science of the Total Environment* **576**, 752–765.
- Meng, J., Li, L., Hao, Z., Wang, J. & Shao, Q. 2014 Suitability of TRMM satellite rainfall in driving a distributed hydrological model in the source region of Yellow River. *Journal of Hydrology* **509** (2), 320–332.
- Moriassi, D. N., Arnold, J. G., Van Liew, M. W., Bingner, R. L., Harmel, R. D. & Veith, T. L. 2007 Model evaluation guidelines for systematic quantification of accuracy in watershed simulations. *Transactions of the ASABE* **50** (3), 885–900.
- Nash, J. E. & Sutcliffe, J. V. 1970 River flow forecasting through conceptual models part I – A discussion of principles. *Journal of Hydrology* **10** (3), 282–290.
- Park, D. & Markus, M. 2014 Analysis of a changing hydrologic flood regime using the Variable Infiltration Capacity model. *Journal of Hydrology* **515** (515), 267–280.
- Plouffe, C. C. F., Robertson, C. & Chandrapala, L. 2015 Comparing interpolation techniques for monthly rainfall mapping using

- multiple evaluation criteria and auxiliary data sources. *Environmental Modelling & Software* **67** (C), 57–71.
- Prakash, S., Mitra, A. K., Momin, I. M., Pai, D. S., Rajagopal, E. N. & Basu, S. 2015 Comparison of TMPA-3b42 versions 6 and 7 precipitation products with gauge-based data over India for the southwest monsoon period. *Journal of Hydrometeorology* **16** (1), 346–362.
- Rui, H. 2010 Tropical rainfall measuring mission (TRMM). *Journal of Atmospheric and Oceanic Technology* **15** (3), 809–817.
- Salio, P., Hobouchian, M. P., Skabar, Y. G. & Vila, D. 2015 Evaluation of high-resolution satellite precipitation estimates over Southern South America using a dense rain gauge network. *Atmospheric Research* **163**, 146–161.
- Saxton, K. E. & Rawls, W. J. 2006 Soil water characteristic estimates by texture and organic matter for hydrologic solutions. *Soil Science Society of America Journal* **70** (5), 1569–1578.
- Siddique-E-Akbor, A. H. M., Hossain, F., Sikder, S., Shum, C. K., Tseng, S., Yi, Y., Turk, F. J. & Limaye, A. 2014 Satellite precipitation data-driven hydrological modeling for water resources management in the Ganges, Brahmaputra, and Meghna basins. *Earth Interactions* **18** (17), 1–25.
- Simpson, J., Kummerow, C., Tao, W. K. & Adler, R. F. 1996 On the tropical rainfall measuring mission (TRMM). *Meteorology and Atmospheric Physics* **60** (1), 19–36.
- Sun, R., Yuan, H., Liu, X. & Jiang, X. 2016 Evaluation of the latest satellite-gauge precipitation products and their hydrologic applications over the Huaihe River basin. *Journal of Hydrology* **536**, 302–319.
- Tang, G., Long, D. & Hong, Y. 2016 Systematic anomalies over inland water bodies of High Mountain Asia in TRMM precipitation estimates: no longer a problem for the GPM era? *IEEE Geoscience and Remote Sensing Letters* **99** (13), 1762–1766.
- Teegavarapu, R. S. V., Meskele, T. & Pathak, C. S. 2012 Geo-spatial grid-based transformations of precipitation estimates using spatial interpolation methods. *Computers & Geosciences* **40** (3), 28–39.
- Tesemma, Z. K., Wei, Y., Peel, M. C. & Western, A. W. 2015 The effect of year-to-year variability of leaf area index on Variable Infiltration Capacity model performance and simulation of runoff. *Advances in Water Resources* **83** (9), 310–322.
- Tong, K., Su, F., Yang, D. & Hao, Z. 2014 Evaluation of satellite precipitation retrievals and their potential utilities in hydrologic modeling over the Tibetan Plateau. *Journal of Hydrology* **519**, 423–437.
- Torgo, L. 2017 *Data Mining with R: Learning with Case Studies*, 2nd edn. Chapman & Hall/CRC, Boca Raton, FL.
- Wang, Z., Zhong, R. & Lai, C. 2017a Evaluation and hydrologic validation of TMPA satellite precipitation product downstream of the Pearl River Basin, China. *Hydrological Processes* **31**, 4169–4182.
- Wang, Z., Zhong, R., Lai, C. & Chen, J. 2017b Evaluation of the GPM IMERG satellite-based precipitation products and the hydrological utility. *Atmospheric Research* **196**, 151–163.
- Wang, Z., Zhong, R., Lai, C., Zeng, Z., Lian, Y. & Bai, X. 2018 Climate change enhances the severity and variability of drought in the Pearl River Basin in South China in the 21st century. *Agricultural and Forest Meteorology* **249**, 149–162.
- Xue, X., Hong, Y., Limaye, A. S., Gourley, J. J., Huffman, G. J., Khan, S. I., Dorji, C. & Chen, S. 2013 Statistical and hydrological evaluation of TRMM-based Multi-satellite Precipitation Analysis over the Wangchu Basin of Bhutan: are the latest satellite precipitation products 3b42v7 ready for use in ungauged basins? *Journal of Hydrology* **499** (13–14), 91–99.
- Yang, Y., Cheng, G., Fan, J., Sun, J. & Li, W. 2013 Representativeness and reliability of satellite rainfall dataset in alpine and gorge region. *Advances in Water Science* **24** (1), 24–33 (Chinese with English abstract).
- Yao, J. & Tan, C. L. 2000 A case study on using neural networks to perform technical forecasting of forex. *Neurocomputing* **34** (1–4), 79–98.
- Yong, B., Ren, L., Hong, Y., Wang, J., Gourley, J. J., Jiang, S., Chen, X. & Wang, W. 2010 Hydrologic evaluation of Multisatellite Precipitation Analysis standard precipitation products in basins beyond its inclined latitude band: a case study in Laohahe basin, China. *Water Resources Research* **46** (7), 759–768.
- Yong, B., Chen, B., Gourley, J. J., Ren, L., Hong, Y., Chen, X., Wang, W., Chen, S. & Gong, L. 2014 Intercomparison of the version-6 and version-7 TMPA precipitation products over high and low latitudes basins with independent gauge networks: is the newer version better in both real-time and post-real-time analysis for water resources and hydrologic extremes? *Journal of Hydrology* **508** (2), 77–87.
- Zeng, H. & Li, L. 2011 Accuracy validation of TRMM 3b43 data in Lancang River basin. *Journal of Geographical Sciences* **7**, 994–1004.
- Zeng, H., Li, L. & Li, J. 2012 The evaluation of TRMM Multisatellite Precipitation Analysis (TMPA) in drought monitoring in the Lancang River basin. *Journal of Geographical Sciences* **22** (2), 273–282.
- Zulkafli, Z., Buytaert, W., Onof, C., Manz, B., Tarnavsky, E., Lavado, W. & Guyot, J. 2014 A comparative performance analysis of TRMM 3b42 (TMPA) versions 6 and 7 for hydrological applications over Andean-Amazon River basins. *Journal of Hydrometeorology* **15** (2), 581–592.

First received 30 January 2018; accepted in revised form 16 June 2018. Available online 9 July 2018